The orientation of Langmuir–Blodgett monolayers using NEXAFS

D. A. Outka,[a] J. Stöhr, J. P. Rabe,[b] and J. D. Swalen
IBM Almaden Research Center, San Jose, California 95120-6099

(Received 29 May 1987; accepted 2 December 1987)

Carbon *K*-shell NEXAFS (near edge x-ray absorption fine structure) spectra of oriented hydrocarbon chains in Langmuir–Blodgett (LB) monolayers were measured and used to study the orientation of these molecules. The LB monolayers were assembled from arachidic acid or cadmium or calcium arachidate on the oxidized Si(111) surface. The observed NEXAFS resonances are assigned to transitions to excited states which are localized on individual CH_2 groups or C–C bonds. From a detailed analysis using curve-fitting techniques of the angular dependence of the various spectral peaks, the hydrocarbon chains of the cadmium arachidate monolayer is estimated to lie within 15° of the surface normal, the hydrocarbon chains of the calcium arachidate monolayer is estimated to be tilted by $33 \pm 5°$ from the surface normal, while the arachidic acid monolayer is not ordered at all. The determined chain orientations are discussed in terms of a microscopic model involving lateral interactions between the zig–zag hydrocarbon chains.

I. INTRODUCTION

Ultrathin organic films can be deposited on solid surfaces by the Langmuir–Blodgett technique,[1,2] a method which allows the formation of well defined monomolecular layers, each on the order of 3 nm thick. Typically these films consist of long hydrocarbon chains ($\gtrsim C_{12}$) terminated at one end by a carboxylic acid group ($-CO_2H$) or the salt ($-CO_2^-$). Under appropriate conditions (*p*H and temperature) a monolayer or multilayer LB film can be transferred to a solid surface by successive dipping of a substrate through a compressed layer of molecules on a water surface. These films are highly ordered with parallel hydrocarbon chains. Numerous applications of these films have been discussed[3] including use in microlithography, electrooptics, biochemical sensing, and tribology. Essential for a system design, however, is a detailed characterization of the molecular structure of the film. A range of techniques have been adapted for this purpose from the early optical measurements of the indices of refraction and interference patterns[1] to more recent infrared[4] and Raman[5] spectroscopies; electron[6] and x-ray[7] diffraction; and scanning tunneling microscopy.[8] Single monolayers are, however, still relatively difficult to examine. NEXAFS (near edge x-ray absorption fine structure) is a nondestructive synchrotron radiation based technique which has been shown to be useful in examining the orientation and bonding of small chemisorbed molecules[9,10] and therefore should be ideally suited to study larger molecules such as LB films.

In the NEXAFS technique, a *K*-shell electron is excited to unoccupied orbitals near the ionization threshold. Since the properties of these unoccupied orbitals, in molecules, are determined to some extent by the bonding in the molecule, NEXAFS is sensitive to certain molecular properties. For example, NEXAFS can identify transitions to the following empty states C–C σ^*, C=C σ^*, C=C π^*, C≡C σ^*, C≡C π^*, C–O σ^*, C=O σ^*, C=O π^*, C≡O σ^*, and C≡O π^*. With this technique the presence of these groups and their orientation relative to the surface can be determined.

In this study, the NEXAFS technique is extended beyond simple molecular adsorption systems and applied to hydrocarbon chains in single layer LB films on an oxidized Si(111) surface. The LB layers studied were arachidic acid [$CH_3(CH_2)_{18}CO_2H$] and cadmium and calcium arachidate. The latter two form films with oriented hydrocarbon chains which NEXAFS is readily able to discern. The NEXAFS spectra of all of these are found to be similar to those of small hydrocarbon molecules and the peaks interpreted in terms of resonances with excited states localized on individual CH_2 groups or C–C bonds. From the angular dependence of these NEXAFS peaks the orientations of the hydrocarbon chains in the particular cadmium and calcium arachidate films examined are determined to be tilted by 0° and 33°, respectively.

One of the major foci of this work will be the development of procedures for the *quantitative* analysis of NEXAFS spectra. This includes least-squares fitting of the NEXAFS spectra and a consideration of the line shapes of the various near-edge features. When possible, physical interpretations of the line shapes and the parameters derived from the fitting procedure will be presented, but the overall approach of this study is empirical. The hope is that this more quantitative approach will provide a basis for future theoretical consideration of the line shapes and parameters which describe NEXAFS spectra.

The organization of this paper is as follows. The details of the experimental apparatus and conditions are presented in Sec. II. In Sec. III the NEXAFS spectra of various hydrocarbon containing molecules will be compared and the peaks assigned to specific transitions. The analysis of NEXAFS spectra is split into two sections with the first, Sec. IV A, devoted to analyzing the angle-dependent components of the NEXAFS spectra which are isolated by forming difference spectra. This analysis consists of least-squares fits to the data and interpretation of the angular dependence of x-ray ab-

[a] Present address: Sandia National Laboratories, Division 8343, Livermore, CA 94550.
[b] Present address: Max-Planck-Institut für Polymerforschung, Postfach 3148, D-6500 Mainz, Federal Republic of Germany.

 0021-9606/88/064076-12$02.10

sorption by various physical models for the geometry of the hydrocarbon chains on the surface. The second data analysis, Sec. IV B, considers how the angle-dependent and isotropic components of the NEXAFS spectra combine to form the complete spectra. This is performed again by least-squares fitting and comparison to various physical models. In Sec. V the results are discussed in terms of a microscopic model of surface-bonding and interchain interaction effects. Our results are compared to that of other NEXAFS studies on related molecules and to studies of LB films using other techniques. Conclusions are drawn in Sec. VI.

II. EXPERIMENTAL DETAILS

The experiments were performed on beam line I-1 at the Stanford Synchrotron Radiation Laboratory with the use of a grasshopper monochromator (1200 lines/mm holographic grating). Details of the beam line and data acquisition technique have been previously published.[9,11] The NEXAFS spectra were obtained by total electron yield detection. The x-ray incidence angle was varied from 20° incidence (E near surface normal) to normal incidence (E in surface plane). The energy scale was calibrated using the carbon contaminants on the optical surfaces of the monochromator which have two major absorption peaks at 284.7 and 291.0 eV. The spectra were divided by the signal from a gold grid reference monitor in order to correct for the transmission function of the monochromator.

The three LB films which were analyzed were chosen because they represented a variety of orientations for monolayer LB films ranging from the hydrocarbon chain being normal to the surface, tilted, or disordered. These differences in orientation are likely the result of the conditions during film preparation and do not represent the only orientation possible for these assemblies. That is, a different combination of *p*H, concentration, or just a better transfer from solution (in the case of the arachidic acid film) may result in a different orientation for these assemblies. Single layer LB films were prepared in air on silicon substrates. The silicon wafers were first dipped in Buffered Oxide Etch (J. T. Baker, Phillipsburg, NJ) in order to remove the native oxide along with contaminants. Since the LB films were prepared in air, however, the oxide growth is expected to have partially regrown. Immediately preceding the transfer of the LB monolayer, the wafer was further cleaned with a solution of No Chro Mix Water (Barnstead, Nanopure grade) and dried in nitrogen flow. Arachidic acid (Lachat Chemicals, Mequon, WI) was used as received. The LB monolayers were prepared on a commercially available film balance (Joyce Loebl) with a solid Teflon trough instead of the originally supplied glass tank. The solutions used to prepare the LB films were: Nanopure water at a *p*H of 5.8 for the arachidic acid film; 2.5×10^{-4} mol ℓ^{-1} $CdCl_2$ maintained at a *p*H between 7 and 8 with a Na_2CO_3 buffer for the cadmium arachidate film; and 1×10^{-4} mol ℓ^{-1} $CaCO_3$ maintained at a *p*H between 7 and 8 for the calcium arachidate film. The transfer pressure used was 30 mN m^{-1}.

For the NEXAFS measurement the samples were placed in a stainless steel vacuum chamber which was evacuated (without baking) to 1×10^{-8} Torr. The Langmuir–Blodgett films were quite stable since measurements on some of the samples repeated 6 months later showed little change. Also, no radiation damage effects were observed at the photon fluxes ($\simeq2\times10^{9}$ photons s^{-1}) used in the present experiments.

III. EXPERIMENTAL RESULTS

The carbon core-level excitation spectrum of a molecule containing a hydrocarbon chain exhibits several features which are characteristic of hydrocarbons and which do not greatly depend upon the precise environment in which the hydrocarbon chain is located. For example, the carbon core-level excitation spectra of a variety of molecules containing hydrocarbon chains including gas phase hexane,[12] several LB films on oxidized Si(111) surfaces, and a thin polyethylene film on Si(111), are presented in Fig. 1, and in each case, three pronounced resonances are observed which are characteristic of hydrocarbon chains. The first and lowest energy resonance occurs at 287–289 eV and is attributed to a transition to antibonding orbitals involving the C–H bonds. This assignment is based upon comparison to the core excitation spectra of cyclic[13] and linear[12] hydrocarbons where such an assignment was originally proposed, and from studies of oriented polyethylene and chemisorbed hydrocarbons.[14] This assignment is further supported by the angular dependence of this peak for the oriented chains examined in this study

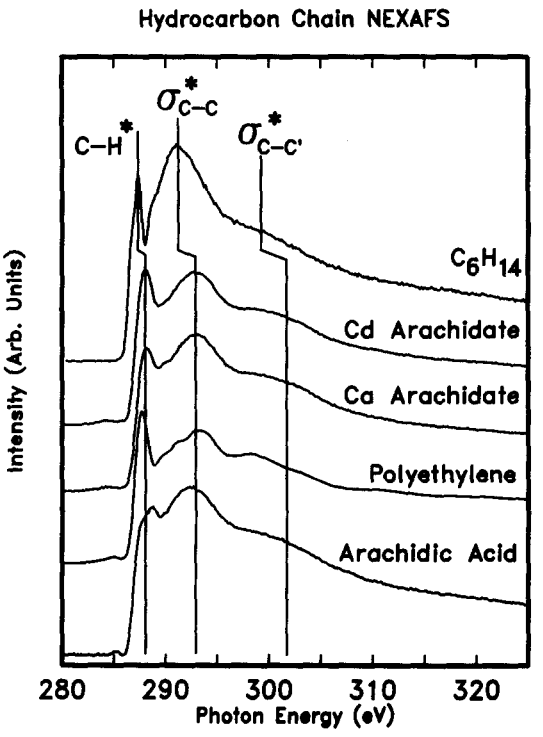

FIG. 1. The carbon *K*-edge excitation spectra of various molecules containing hydrocarbon chains are similar despite differences in environment. All of the spectra show three peaks characteristic of hydrocarbons. The top spectrum is the electron impact excitation spectrum of gaseous *n*-hexane (Ref. 12). The remaining are NEXAFS spectra from this study. To minimize angular effects, the NEXAFS spectra were taken at an x-ray incidence angle of 50°. The polyethylene sample consisted of a thin polyethylene film on a silicon wafer which showed preferential orientation of the chains perpendicular to the surface.

which is discussed in detail below. The second resonance characteristic of hydrocarbons occurs at 291–293 eV and is assigned to a transition to the σ^* orbital of the C–C bonds. The position and width of this resonance is typical of C–C single bonds.[10] The origin of the third resonance which occurs at 300–302 eV is presently not understood, but as shown in Fig. 1, has been observed before in the carbon K-edge spectra of gaseous alkanes. We assign it to C–C antibonding orbitals based upon its angular dependence as discussed in detail below and label it as a C–C′σ^* resonance. The similarity between the NEXAFS spectra of the LB films and of polyethylene (Fig. 1) indicate that the spectra of the LB films is dominated by resonances associated with the hydrocarbon chain with little contribution from the terminal carboxylate group. This is expected from the number of carbon atoms contained in the hydrocarbon chain (19) vs the single carbon atom contained in the carboxylate group. Thus, the carboxylate resonances should be approximately 5% of the size of the hydrocarbon resonances. In addition, there is a minor feature in the spectra of the LB films at 284.7 eV which is due to incomplete correction for the transmission function of the monochromator. There is also a minor peak at approximately 285.5 eV in the spectra of polyethylene and the arachidic acid film which is attributed to a graphitic carbon contaminant.

When the hydrocarbon chains are oriented, the intensities of the three principal resonances depend strongly upon the angle of x-ray incidence. This occurs because the x rays produced by the storage ring are approximately 85% polarized in the plane of the orbit,[9] therefore, the intensity of a NEXAFS resonance depends upon the angle between E of the light and the p-orbital component of the final state.[9,15] This is demonstrated in Fig. 2 for the LB film of cadmium arachidate on Si(111). The C–H* resonance is strong under normal x-ray incidence (E parallel to the surface) while the C–C σ^* and C–C′ σ^* resonances are strongest under glancing x-ray incidence (E normal to the surface). For these types of resonances, the NEXAFS peaks are expected to be strongest when E is parallel to the respective bonds, so this angular dependence already indicates that the hydrocarbon chains of the Cd arachidate are roughly oriented with the C–H bonds parallel to the surface and the C–C bonds perpendicular to the surface.

Not all of the samples exhibit the same degree of angular dependence which makes this a useful criterion for detecting the presence and orientation of *oriented* hydrocarbon chains. For example, Fig. 3 compares the angular dependence of the Cd arachidate, Ca arachidate, and arachidic acid films. The top row of Fig. 3 compares the spectra under normal x-ray incidence, the second row compares the spectra under glancing x-ray incidence, and the bottom row compares the result of subtracting the glancing from the normal incidence spectra. This comparison shows that the Cd arachidate exhibits the greatest dependence upon x-ray incidence angle, the Ca arachidate exhibits a somewhat weaker dependence, while the free arachidic acid exhibits almost no angular dependence. These results indicate that the Cd and Ca arachidate films studied have oriented hydrocarbon chains. Furthermore, quantitative analysis in the next section will show that the weaker angular dependence of the Ca arachidate is due to a tilting of its hydrocarbon chain by approximately 33° rela-

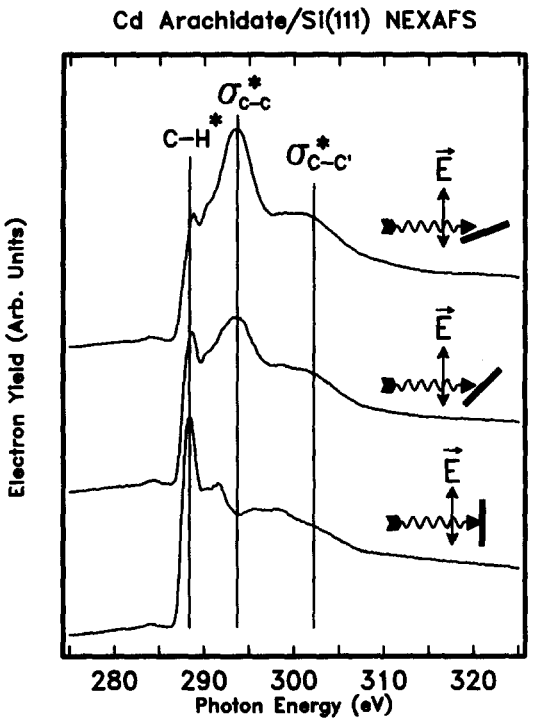

FIG. 2. The carbon K-edge NEXAFS spectra of a cadmium arachidate film on a Si(111) surface at x-ray incidence angles of 20°, 45°, and 90°. The strong angular dependence of the C–H*, C–C σ^*, and C–C′ σ^* resonances indicate that the hydrocarbon chains of this film are oriented near the surface normal.

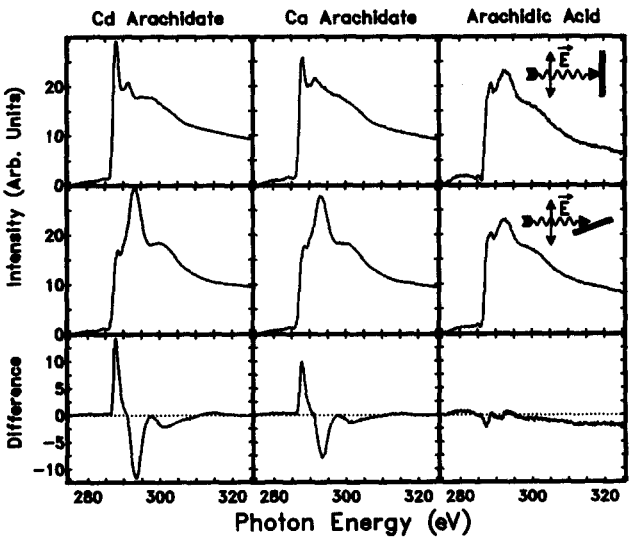

FIG. 3. Comparison of the angular dependence of the NEXAFS spectra of films of cadmium arachidate, calcium arachidate and arachidic acid on a Si(111) surface. The top row shows the spectra near normal x-ray incidence, the second row shows the spectra near a glancing incidence angle, and the bottom row shows the result of subtracting the glancing incidence spectra from the normal incidence spectra. Cadmium arachidate in the first column shows the strongest angular dependence indicating its hydrocarbon chains are nearest the surface normal. The angular dependence of calcium arachidate (second column) is reduced indicating a more tilted geometry. The arachidic acid film (third column) has almost no angular dependence indicating formation of a disordered layer.

tive to the surface normal, whereas the hydrocarbon chain of Cd arachidate is nearly normal to the surface. The absence of an angular dependence for the arachidic acid chain could be due to two possibilities. Either the chains are disordered with no net orientation of the bonds or all of the bonds are fortuitously oriented at the magic angle of 54.7° away from the surface normal.[15] Arguments presented later suggest the former.

IV. NEXAFS SPECTRAL ANALYSIS

A. Analysis of difference spectra

In order to investigate quantitatively the angular dependence of these resonances and thus more precisely deduce the orientations of these LB films, a detailed investigation of the angular dependence of the NEXAFS spectra was undertaken and a mathematical fitting procedure developed to quantify the results. To begin this, a series of NEXAFS spectra of the LB films were measured as a function of the E orientation angle in 10° intervals from 20° to 90° (Figs. 4 and 5). These figures clearly show the pronounced angular dependence of the three principal resonances already mentioned. These figures also show, however, that there is significant structure in the background which must be separated from the angular dependent structure in order to interpret the results quantitatively.

One method of isolating the angular dependent structure in the NEXAFS spectra is to examine the result of subtracting the spectra from each other. These "difference spectra" remove all of the isotropic components of the NEXAFS spectra including the effects of incomplete x-ray polarization, the constant background due to transitions to continuum states, and any other isotropic structure, thereby isolating the angle dependent features. For example, Fig. 6 illustrates the result of subtracting the Cd arachidate spectrum at $\theta = 50°$ from each of the other angles of incidence. Before subtraction, the spectra were scaled to match their values at 275 and 320 eV. The result is the three clearly defined angle-dependent resonances identified earlier which can now be studied in more detail.

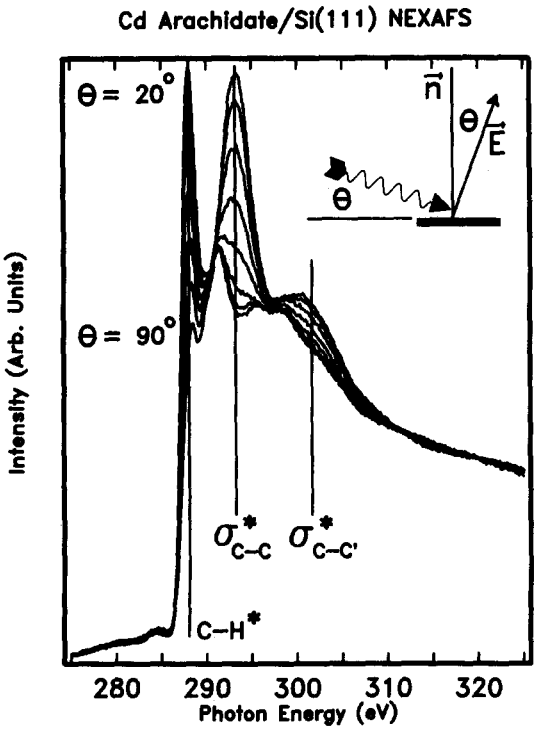

FIG. 4. The carbon K-edge NEXAFS spectra of a cadmium arachidate film on a Si(111) surface at x-ray incidence angles of 20° to 90° in 10° increments.

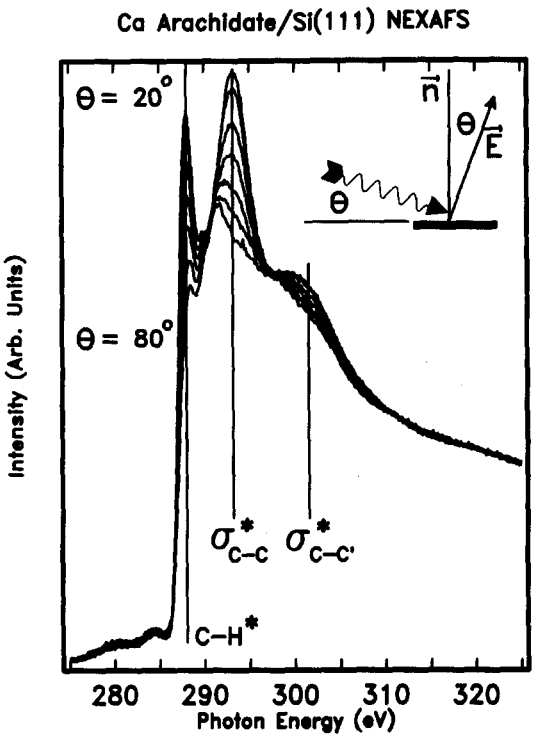

FIG. 5. The carbon K-edge NEXAFS spectra of a calcium arachidate film on a Si(111) surface at x-ray incidence angles of 20° to 80° in 10° increments.

Several aspects of the angular dependent resonances are apparent from an inspection of this series of difference spectra. First, while the intensity of each of these peaks depends strongly upon x-ray incidence angle, the positions and widths do not vary with x-ray incidence angle. Second, the line shapes of each peak do not depend upon the x-ray incidence angle but do differ among the three resonances. For example, the two lowest-energy peaks are nearly symmetrical while the third resonance at 301 eV is noticeably asymmetric with a high energy tail.

In order to quantify these observations the difference spectra were subject to a least-squares fitting procedure as illustrated in Fig. 7. From this procedure a general trend can be identified, which is, the width and a symmetry of a NEXAFS peak increase as its position increases in energy. In general, the resonances below or near the C 1s ionization limit (approximately 291 eV) are well described by a Gaussian line shape while higher energy peaks require an increasingly asymmetric function. For example, Fig. 7 shows that the two lowest energy peaks are well described by a Gaussian line shape. The narrowest peak at 288.0 eV is expected to have a nearly perfect Gaussian line shape because is FWHM (full-width at half-maximum) of 1.6 eV is only slightly larg-

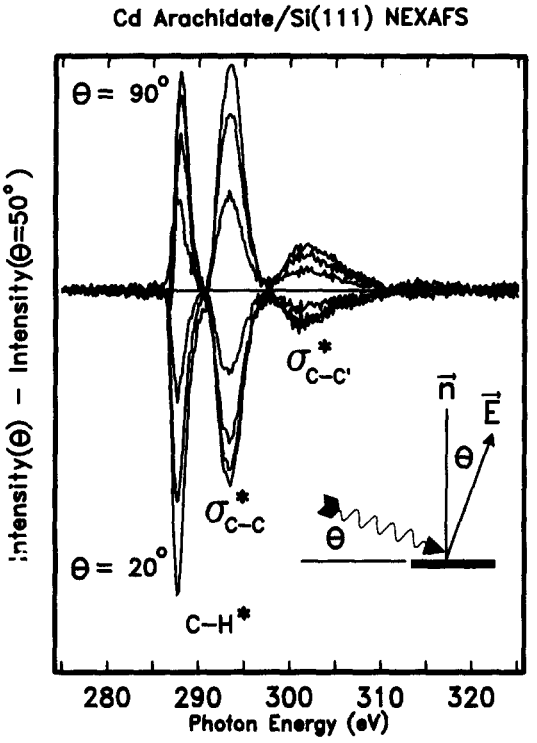

FIG. 6. Difference spectra for a cadmium arachidate film on a Si(111) surface at x-ray incidence angles of 20° to 90° in 10° increments. These difference spectra were obtained by subtracting the original spectrum at a 50° incidence angle from each of the original spectra at the other angles of incidence. This series of difference spectra indicates the three angular dependent NEXAFS peaks.

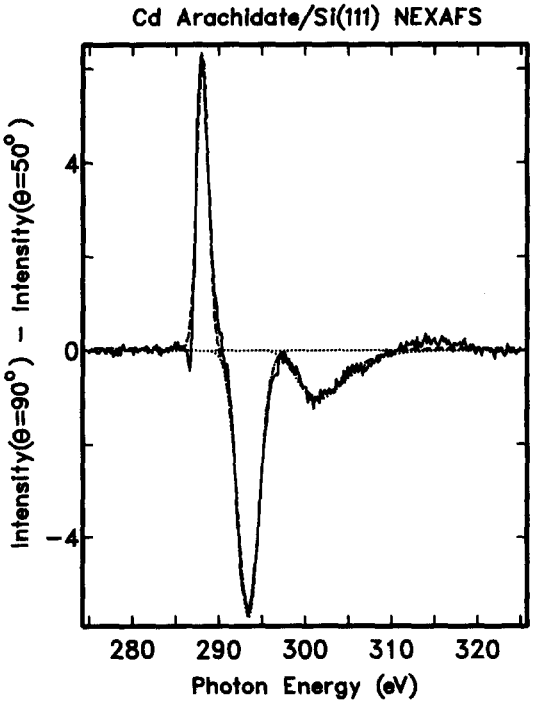

FIG. 7. Difference spectrum for cadmium arachidate film resulting from the subtraction of the spectrum at an x-ray incidence angle of 50° from the spectrum at an x-ray incidence angle of 90°. Superimposed and shown as a dotted line is the least-squares fit of this difference spectrum. The two peaks at lowest energy were fit with normal Gaussian functions while the highest energy peak was fit with an asymmetric Gaussian function.

er than the resolution of monochromator (approximately 1.2 eV). The second resonance at 293.5 eV has a FWHM of 2.9 eV, however, which is considerably larger than the monochromator resolution, yet, it is also well described by a Gaussian function. A slight asymmetry is apparent upon careful inspection, however which is expected from the generalization above. This asymmetry becomes quite obvious for the third resonance located at 301 eV so that an asymmetric function is required to describe it well. Since the source of this asymmetry is not yet understood well enough to describe in mathematical terms based upon a physical model, the third peak was fit to a simple empirically determined function which served the purposes of this study. The function chosen was a modified Gaussian with an energy dependent width. A normal Gaussian peak has the formula

$$I = H \exp\left[\frac{-1}{2}\left(\frac{E-P}{W/c}\right)^2\right], \tag{1}$$

where H is the maximum value of the function; W is the FWHM of the peak; P is the position of the peak; E is the independent variable which in this case is the energy; and c is a constant defined by $c = 2\sqrt{\ln(4)}$. The modified Gaussian used to describe the third asymmetric NEXAFS resonance differs in that W is not constant but depends upon the energy E in a linear manner: $W = (E - 190)m + b$ where $m = 0.3414$ and $b = -30.24$ as determined by the least-squares fit to the data. The functions and parameters just described provide a good fit to all of the difference spectra of Cd arachidate—independent of angle—which justifies the generalization made above that the width and positions of these peaks are independent of E orientation. Furthermore, these same functions and parameters fit the difference spectra of Ca arachidate as well, demonstrating that the NEXAFS features of a hydrocarbon chain do not depend upon the details of its environment.

Since the difference spectra can be fit so well, it is reasonable to analyze the variation in intensity of the various peaks in the difference spectra as a function of E angle, θ, to try to deduce the orientation of the various bonds and hence of the molecules. Unfortunately, examination of the equations covering the angular dependence of NEXAFS resonances reveals that *the absolute orientation of a single layer cannot be determined from its difference spectra alone.* The difference spectra of two similar systems can be compared, however, to discern relative differences in orientation. Since there already exists considerable evidence from vibrational spectroscopy and coverage measurements that the hydrocarbon chain of Cd arachidate is oriented normal to many substrate materials,[4,5] we shall use the relative information from the difference spectra to show that the hydrocarbon chains of Ca arachidate are tilted by $33 \pm 5°$ from the surface normal. The absolute orientation of Cd arachidate will be considered later in the analysis of the original NEXAFS spectra to show that the spectra are consistent with the hydrocarbon chain being normal to the surface.

The equations covering the angular dependence of NEXAFS resonances will be examined first to show why the information about the molecular orientation is lost from the difference spectra of a single sample. The NEXAFS reson-

ances obey dipole selection rules so their intensity depends upon the angle between E of the light and the p component of the antibonding orbital which is involved. Instead of analyzing the angular dependence in this molecular coordinate system, it is easier to make measurements using a laboratory based coordinate system. The basic equations concerning the angular dependence of π^* and σ^* resonances in such a laboratory coordinate system have already been presented in detail elsewhere.[15] As an example, consider a single vector-type orbital such as an isolated C–C σ^* or C–H* orbitals in the molecules of this study. The indensity due to the principal or parallel-polarized component of the x rays for a substrate with threefold or higher symmetry is[15]

$$I^{\parallel}_{\text{vec}} = A\,[\cos^2\theta\cos^2\alpha + \tfrac{1}{2}\sin^2\theta\sin^2\alpha], \tag{2}$$

where θ is the angle between E and the surface normal, α is the angle between the p component of the antibonding orbital and the surface normal, and A is a constant which depends upon the bond involved and the detection geometry.[15] This can be rewritten as

$$I^{\parallel}_{\text{vec}} = A\left[\cos^2\theta(1-\tfrac{3}{2}\sin^2\alpha) + \tfrac{1}{2}\sin^2\alpha\right]. \tag{3}$$

Upon subtracting two spectra for the same orientation of a vector-type orbital but measured at different angles of θ, the final term of Eq. (3) falls out to give

$$I_{\text{vec}}(\theta) - I_{\text{vec}}(\theta_{\text{ref}}) = A\left[1-\tfrac{3}{2}\sin^2\alpha\right]\left[\cos^2\theta - \cos^2\theta_{\text{ref}}\right] \tag{4a}$$

or

$$\frac{I_{\text{vec}}(\theta) - I_{\text{vec}}(\theta_{\text{ref}})}{\cos^2\theta - \cos^2\theta_{\text{ref}}} = S = \text{const.} \tag{4b}$$

In Eq. (4a) the unknown information contained in α and A is separated from the known information regarding the experimental arrangement contained in θ. This is a general phenomenon. Indeed, plots of the intensities of difference spectra peaks for any type of orbital, not just the simple vector-type orbitals considered so far, exhibit the same general dependence on θ shown in Eq. (4b). For example, Fig. 8 plots the areas of the three peaks from the difference spectra of Cd and Ca arachidate as a function of E angle and in all cases the experimental data can be reasonably fit to Eq. (4b) with a difference of only a positive or negative scale factor S. In general, S has two components

$$S = A \times f(\text{geometry}), \tag{5}$$

where f(geometry) is a molecular orientation term and A depends upon instrumental parameters and the x-ray absorption cross section. For the single vector-type orbital considered so far, S is defined by Eqs. (4a) and (4b) such that $f(\text{geometry}) = 1 - \frac{3}{2}\sin^2\alpha$.

While the orientation of a single sample cannot be deduced from its difference spectra without knowing A, the difference spectra of two similar systems can be compared to obtain their *relative* orientation. For example, since Cd and Ca arachidate are so similar and since the same detection apparatus was used in both measurements, the factor A in Eq. (5) for these molecules can be assumed to be the same. If S_{Cd} is divided by S_{Ca}, the factors of A cancel, and an expression relating the geometries of the two molecules is obtained:

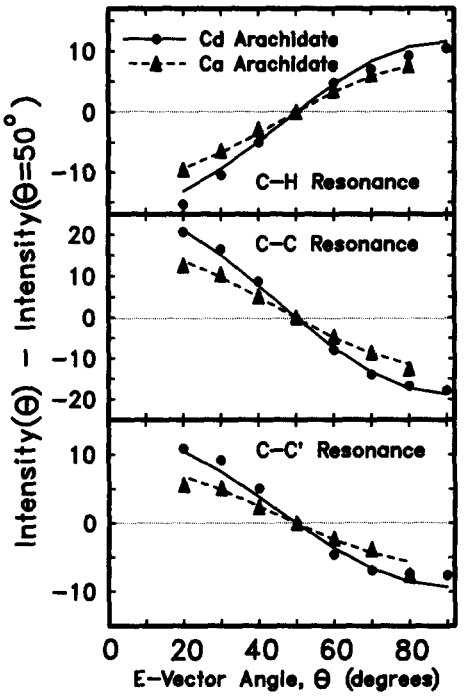

FIG. 8. These plots compare the intensities of the three peaks in the difference spectra of Cd arachidate vs the intensities of the same three peaks of Ca arachidate. For all three peaks, the angular dependence is greater for Cd arachidate than for Ca arachidate. Also shown are fits of the data points to Eq. (4b) showing that all of these resonances exhibit the same functional dependence upon E-vector angle, θ.

$R = S_{\text{Ca}}/S_{\text{Cd}} = f_{\text{Ca}}/f_{\text{Cd}}$. The ratio R derived by fitting the experimental data to Eq. (4b) as shown in Fig. 8 are: $R = 0.710$ for the C–H* resonance, $R = 0.652$ for the C–C σ^* resonance, and $R = 0.656$ for the C–C' σ^* resonance.

The values for the C–C and C–C' σ^* resonances are quite similar indicating that the angular dependence for these resonances are the same. This forms the basis for identifying the third resonance at 301 eV as related to the C–C bonding. The ratio R for the C–H* resonance, however, is significantly different. This is because the C–H orbitals make a different angle with the surface normal than the C–C orbitals. In order to interpret these R values in terms of relative geometries of the two LB films, Eq. (5) needs to be adapted by a model which takes into account the details of the geometry of the hydrocarbon chains and the polarization dependence of x-ray absorption.

The model which we propose for the LB chains on silicon is referred to as the "tilted-chain" model (Fig. 9). This model averages over various domains so there is no net azimuthal orientation. Each individual hydrocarbon chain in this model is assumed to tilt only in the plane containing the C–C–C bonds and have an all *trans* geometry. Furthermore, the C–C bonds are treated as isolated vector-type orbitals as in Eq. (4a), but each hydrocarbon chain has *two* C–C bonds which make two different angles with E. Of course, if the chain is normal to the surface and the C–C–C bond angles are 115° [16] then both C–C bonds make an angle of 32.5° with the surface normal ($\alpha = 32.5°$) and Eq. (4a) could be used directly. If the chain is tilted, however, then the two C–C bonds make different angles with the surface normal and Eq.

(4a) cannot be used directly. Since there is a geometric relationship between the two C–C bonds, however, the equation for a single orbital (4a) can be adapted to the case of a hydrocarbon chain with an arbitrary tilt angle. First, the contributions of the two C–C bonds described by Eq. (4a) are added together. Then the molecular geometry factors can be factored out so the geometric dependence is of the form

$$f_{\text{tilt}}^{\text{C-C}}(\alpha_{\text{CC1}}, \alpha_{\text{CC2}}) = f(\alpha_{\text{CC1}}) + f(\alpha_{\text{CC2}}) = [1 - \tfrac{3}{2}\sin^2 \alpha_{\text{CC1}}] + [1 - \tfrac{3}{2}\sin^2 \alpha_{\text{CC2}}], \quad (6a)$$

where α_{CC1} and α_{CC2} are the angles between the two individual C–C bonds and the surface normal. Changing to more convenient coordinates yields

$$f_{\text{tilt}}^{\text{C-C}}(\tau) = 1 - \tfrac{3}{4}[1 + \cos \delta_{\text{CCC}} \cos 2\tau], \quad (6b)$$

where τ is the tilt angle of the chain from the surface normal and δ_{CCC} is the C–C–C bond angle. Note, that this equation predicts the C–C σ^* resonance to be isotropic only if the hydrocarbon chain is tilted by approximately 71°.

Combining the experimental observations with the tilted-chain model, Eq. (6b), implies that the Ca arachidate hydrocarbon chain is tilted significantly more than the Cd arachidate chain. This is deduced from the average ratio, $S_{\text{Ca}}/S_{\text{Cd}} = 0.654$ measured for the C–C and C–C′ σ^* resonances. Assuming that the hydrocarbon chain of Cd arachidate is oriented normal to the surface and that $\delta_{\text{CCC}} = 115°$, implies that the hydrocarbon chain of Ca arachidate is tilted by 33.8°.

The C–H* resonances can also be analyzed using the tilted-chain geometry to yield a tilt angle of 32.8° for the hydrocarbon chain of Ca arachidate. Because the geometry of the C–H bonds differs from the C–C bonds, the C–H* resonance gives a measure of the relative tilting of the Ca and Cd arachidate chains which is independent of the C–C resonances. In this analysis we shall assume that the p component of the two C–H antibonding orbitals is directed along the C–H bonds. This geometry for the C–H* orbitals is also valid for linear combinations of the two C–H* orbitals which have been invoked in certain cases,[14] provided the two components of C–H* orbitals have the same energy. This appears to be satisfied in this case since the position of the C–H* resonance does not vary with changes in the orientation of E. The starting point for describing the C–H orbitals is the vector-type orbital whose NEXAFS angular dependence is given in Eq. (4a). In the limiting case of the hydrocarbon chains being normal to the surface, the C–H bonds are parallel to the surface and $\alpha^{\text{C-H}} = 90°$. As the chain tilts $\alpha^{\text{C-H}}$ decreases, but not identically with the tilt angle. Using the same tilted-chain geometry as above, the relationship between the tilt of the hydrocarbon chain, τ, and $\alpha^{\text{C-H}}$ (the angle the C–H bonds make with the surface normal) is

$$\alpha_{\text{tilt}}^{\text{C-H}}(\tau) = \arccos\left(\frac{\sin \tau}{\sqrt{1 + \tan^2(\delta_{\text{HCH}}/2)}}\right), \quad (7)$$

where δ_{HCH} is the HCH bond angle. Combining this equation with Eq. (4a) yields a relationship between the intensity of the C–H* resonance in the difference spectra and the tilt of hydrocarbon chain:

$$f_{\text{tilt}}^{\text{C-H}}(\tau) = 1 - \tfrac{3}{4}[1 - \cos 2\tau + \cos \delta_{\text{HCH}} - \cos 2\tau \cos \delta_{\text{HCH}}], \quad (8)$$

where τ is the tilt angle of the chain from the surface normal. Using $\delta_{\text{HCH}} = 110°$ and the experimental observation that $S_{\text{Ca}}^{\text{C-H}}/S_{\text{Cd}}^{\text{C-H}} = 0.710$ yields a tilt of 32.8° for the Ca arachidate assuming the Cd arachidate is normal to the surface. This differs by only a degree from the 33.8° value obtained from the C–C and C–C′σ^* resonances with the tilted-chain model so the data from the C–H, C–C, and C–C′ resonances are remarkably consistent.

Although the tilted-chain model is the favored model for the LB films for reasons discussed later, several other models were considered and each predicts the Ca arachidate chain to be more tilted than the Cd arachidate chain. For example, another geometric model for the hydrocarbon chains is called the "spinning-chain" model and is illustrated in Fig. 9. This model is so-called because the hydrocarbon chains are allowed to spin about their axis rather than just tilt in the CCC plane. In this case the C–H* orbitals can be treated like a plane[15] and the equation for f(geometry) becomes rather simple:

$$f_{\text{spin}}^{\text{C-H}}(\gamma) = [1 - \tfrac{3}{2}\sin^2 \gamma], \quad (9)$$

where γ is the tilt angle of the C–H plane as measured by the angle between the normal to the C–H plane and the surface normal. In this case $\gamma = \tau$. Using Eq. (9) the tilt of Ca arachidate becomes 25.4° assuming that the Cd arachidate chain is normal to the surface and $\delta_{\text{CCC}} = 115°$.

A similar tilt is determined from the C–C and C–C′σ^* resonances using the spinning-chain model. The C–C bonds transcribe a cone as the chain spins so the equation for $f_{\text{spin}}^{\text{C-C}}$ of the C–C and C–C′σ^* resonances is

$$f_{\text{spin}}^{\text{C-C}}(\tau) = \frac{-1}{2} + \frac{3}{2}\cos^2\left(90° - \frac{\theta_{\text{CCC}}}{2}\right)\cos^2 \tau. \quad (10)$$

From the average measured ratio of 0.654, the tilt of the Ca arachidate becomes 24.7° assuming that the chain of the Cd arachidate is normal to the surface. This value is consistent with the chain tilt of 25.4° obtained from the C–H orbitals using the same spinning-chain model, but is about 8° less than the tilted-chain model.

Finally, we considered a second possible model for x-ray absorption by the C–C bonds which we call the "C–C interaction model". This model assumes that interaction among

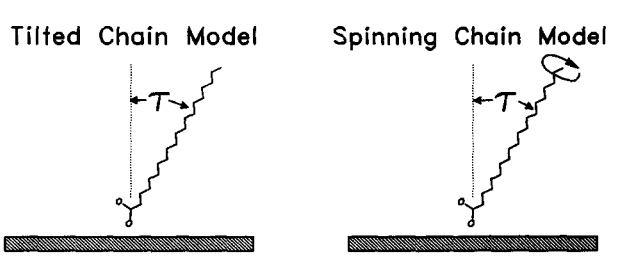

FIG. 9. Comparison of the tilted-chain geometry with the spinning-chain model. The tilted-chain model allows the hydrocarbon chains to tilt only in the C–C–C plane. Individual chains are immobile, but because of different domains there is no net azimuthal orientation. The spinning-chain model is similar but the chains are allowed to rotate about the axis.

two adjacent C–C antibonding orbitals forms two new antibonding orbitals which are directed parallel and perpendicular to the chain direction. The reason this model was originally considered, and later rejected, will be discussed in detail later, but basically it was because the strong angular dependence of the C–C σ^* resonance in Cd arachidate (Fig. 2) suggested that the C–C antibonding orbital had to be directed exactly along the chain direction rather than along the individual C–C bonds. If this model were followed and only the contribution of the antibonding orbital parallel to the chain is considered, the angular dependence of the C–C resonance is like a simple vector orbital described in Eq. (4a) where α is the same as the tilt angle τ. The tilt of the Ca arachidate is then estimated to be 28.7°, assuming that the Cd arachidate is normal to the surface. In this model the C–H* resonance intensities could lead to either 25.4° by use of the spinning chain or 32.8° by use of the tilted-chain model. Therefore, there is an inconsistency of the tilt angles derived from the C–C σ^* and C–H* resonances in this model.

B. Analysis of original spectra

From the difference spectra only the orientation of a molecule relative to a similar molecule can be obtained. For example, the previous section showed that the hydrocarbon chain of the Ca arachidate was tilted by 25.4° to 33.8° (depending upon the model used) relative to Cd arachidate assuming the chain of the latter was oriented normal to the surface. In order to determine the absolute orientations of either Ca or Cd arachidate, however, one must analyze the original spectra. In this section the original NEXAFS spectra for the Cd arachidate film will be analyzed using a fitting procedure. The results indicate that the hydrocarbon chain of Cd arachidate is, indeed, oriented normal to the surface.

The second reason to analyze the original NEXAFS spectra is to show that the angular dependence of the C–C σ^* resonance can be explained by noninteracting C–C antibonding orbitals. This is contrasted with the C–C interaction model mentioned above in which there is interaction between adjacent C–C antibonding orbitals to form two new orbitals which are parallel and perpendicular to the hydrocarbon chain direction. The reason why it was ever considered in the first place is that in the series of original spectra for Cd arachidate in Fig. 4, the C–C σ^* resonance appears to *disappear entirely* at normal x-ray incidence (see also Fig. 2). This is not possible, however, for x-ray absorption by noninteracting C–C bonds of a hydrocarbon chain because the 115° C–C–C bond angle means there is always a projection of E onto one of the C–C bonds. Thus it seemed from the NEXAFS spectra that interaction of the C–C antibonding orbitals must have occurred to form new antibonding orbitals which are parallel and perpendicular to the hydrocarbon chain. This was entirely plausible since such interaction does occur in excitations of the *valence* orbitals of hydrocarbons.[17,18] The analysis of the original NEXAFS spectra in this section will demonstrate that, with reasonable assumptions regarding the background and despite the appearance of the spectra, the angular dependence of the C–C σ^* resonance is consistent with noninteracting C–C antibonding orbitals. Furthermore, the C–C interaction model was deficient in that no resonance could be found to correspond to the antibonding orbital perpendicular to the chain.

The original spectra are composed of several features, some of which depend upon angle some of which do not. The angle-dependent features have already been identified from the difference spectra as regards their position and widths. Their absolute intensities are not known, however. The isotropic features, of course, fall out of the difference spectra so are not yet characterized. They can be divided into two groups, however, one final state which represents transitions to the *continuum* and a group of states which represent transitions to *discrete* states. The approach in this paper will be to provide a mathematical function for transitions to the first type of final state, the continuum, and then use a subtraction procedure to eliminate the remaining discrete final states.

The first step is to insert the mathematical functions for the angular dependent peaks and create a function to describe the step in the spectrum which occurs because of transitions to the continuum states. Figure 10 illustrates the result of this process by showing the normal x-ray incidence Cd arachidate spectrum with the selected mathematical functions superimposed. The positions and widths of the three peaks in the top graph were exactly those obtained from the difference spectra. Also shown is a step-like function which represents the transitions to the continuum. There have been previous attempts to functionalize this step,

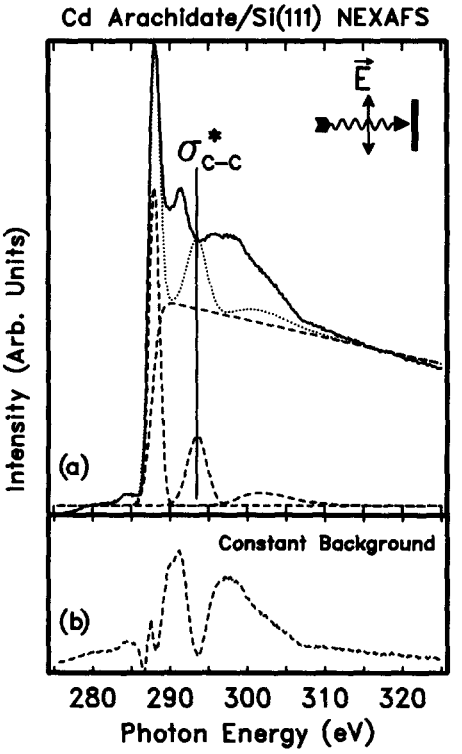

FIG. 10. This diagram shows how the original spectrum for cadmium arachidate at normal x-ray incidence [solid line in (a)] is composed of three angular dependent peaks and the x-ray absorption step [individual features are dashed and the sum is dotted in (a)] and an isotropic background [shown in (b)]. The size of the C–C σ^* resonance shown here is just large enough to be consistent with a hydrocarbon chain normal to the surface and with noninteracting C–C antibonding orbitals.

for example, in the study of the C 1*s* edge of diamond by Morar *et al.*[19] and in the study of the $L_{2,3}$ near-edge region of Pt and Ir compounds by Horsley.[20] In these studies the step was represented by the integral of a Lorentzion function which is an arctan function. The error function was chosen in this work to represent the transitions to the continuum because this function is the result of a convolution of a vertical step with the Gaussian output of the monochromator. A linearly decaying background was also added to represent the decay which is normally observed in x-ray absorption spectra above the edge:

$$I_{\text{step}} = H\left[\frac{1}{2} + \frac{1}{2}\,\text{erf}\left(\frac{E-P}{W/c}\right)\right], \quad E \leqslant P + W, \quad (11a)$$

$$I_{\text{step}} = H\left[\frac{1}{2} + \frac{1}{2}\,\text{erf}\left(\frac{E-P}{W/c}\right)\right] + d\,(E - P - W), \quad E > P + W, \quad (11b)$$

where H is the height of the function immediately above the step, P is the position of the inflection point of the step, E is the independent variable which in this case is energy, W is the FWHM of the step, c is a constant defined by $c = 2\sqrt{\ln(4)}$, and d is the linear decay in the region above the step. The linear decay was established by a fit to the flattest region above the step which occurs between 315 to 325 eV in the glancing incidence spectra.

Although the positions and widths of angle-dependent NEXAFS peaks can be obtained from the difference spectra, their intensities cannot be so easily derived and, indeed, obtaining the intensities is the principal difficulty in analyzing the original spectra. The reason the intensities are so hard to determine is that the exact shape of the background is unknown. For example, examination of the outlines formed by the series of original spectra of Cd and Ca arachidate in Figs. 4 and 5 suggests a background with considerable structure. Since one of the purposes of analyzing the original spectra is to show that the C–C σ^* resonance is consistent with noninteracting C–C antibonding orbitals, the height of the C–C σ^* resonance will be set so that it tests this assumption. This is accomplished if the C–C σ^* resonance at 293.5 eV is maximized under normal x-ray incidence using a linear background as shown in Fig. 10.

This test of the original NEXAFS spectra demonstrates that they are consistent with noninteracting C–C antibonding orbitals. With the intensity of the C–C σ^* resonance set as shown in Fig. 10, the intensities of the C–C σ^* resonance at 301 eV and the C–H* resonance at 288.2 eV were then fixed in this normal incidence spectrum so that they were consistent with the angular dependence of the 293.5 eV peak (Fig. 10). While the angular-dependent resonances and the continuum states can be easily fit to a mathematical model, the remaining isotropic discrete states cannot. Instead of trying to parametrize the remaining isotropic states they will simply be obtained by subtracting the mathematically described states from the original spectra. This "constant background" obtained by subtracting the calculated dotted curve in Fig. 10 from the experimental spectrum is shown at the bottom of Fig. 10 and resembles the background outlined by the curves in Figs. 4 and 5. This constant background was subtracted from each of the spectra at the other angles of x-ray incidence and the result least-squares fit to the remaining mathematical functions. The resultant intensity variation of the three angle dependent peaks are shown in Fig. 11 which plots the *absolute* intensity of the C–H*, C–C σ^*, and C–C′ σ^* resonances vs the polar angle between E and the surface normal. Also shown is the calculated intensity of these peaks using the assumptions of the tilted-chain model described above as the hydrocarbon chain tilts by 0°, 10°, 20°, and 30° from the surface normal. The calculated intensities of the C–C and C–C′ σ^* resonances are obtained by summing the result of Eq. (2) for the two C–C bonds as the chain tilts. The effects of 85% x-ray polarization[9] are also accounted for as described elsewhere.[15] The calculated intensity of the C–H* resonances also uses Eq. (2) combined with Eq. (7) to convert from $\alpha_{\text{C-H}}$ coordinates to τ which is the more convenient tilt of the hydrocarbon chain. The plot of Fig. 11 shows that the angular variation of the C–C σ^* resonance is just great enough for the hydrocarbon chain of Cd arachidate to be normal to the surface, and shows that the C–C′ σ^* and C–H* resonances can also be made consistent with this model. The importance of Fig. 11 is that it shows that the angular dependence of the three variable NEXAFS peaks can be made consistent with noninteracting C–C antibonding orbitals using reasonable assumptions regarding the background and other parameters.

Although the constant background which was subtracted out of the spectrum of Fig. 10 cannot be assigned definitively to specific final states, there are a number of possibili-

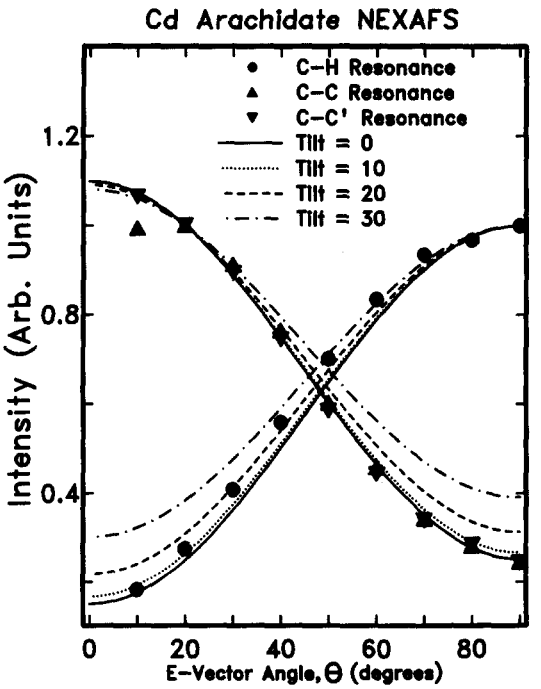

FIG. 11. Plots of the areas of the C–H*, C–C σ^*, and C–C′ σ^* resonances obtained from fits of the original Cd arachidate spectra after subtracting the isotropic background of Fig. 10 from each spectrum. The angular dependence of the C–C σ^* resonance, in particular, is just great enough to be consistent with a hydrocarbon chain oriented normal to the surface assuming that the tilted-chain model applies with its noninteracting C–C orbitals. The angular dependences of the C–H* and C–C′ σ^* resonances are also consistent with this model.

ties for the source of this structure. For example, part of the peak stretching from 296 to 303 eV is certainly due to the carboxylate group of the arachidate. In particular, resonances of the C–O and C=O σ^* bonds are expected in this region by comparison to formic acid which has such features at 297.5 and 301.4 eV.[21] Note, that if the carboxylate groups are ordered then their NEXAFS features might exhibit an angular dependence. The carboxylate group contributes only 1 out of 20 of the carbon atoms of the arachidic acid molecule, however, so the overall intensity of these features are expected to be relatively small, therefore, the angular dependence of them has been ignored. Since the LB films were prepared in air there may also be some contamination of carbon or organics adsorbed on the silicon surface or on top of the LB layer which would contribute to this constant background. Finally, some of this constant background may be due to final states resulting from the electronic band structure of these long hydrocarbon chain molecules. This is supported by the close resemblance of the LB film spectra and those for polyethylene.[22]

V. DISCUSSION

This study finds a distinct difference in the orientations of the hydrocarbon chains of Cd and Ca arachidate on the Si(111) surface. In particular, the tilt angles are estimated to be 0° and 33° from the surface normal, respectively, as illustrated in Fig. 12. There is a simple geometric argument which can account for the stability of these two orientations. Referring to the bottom of Fig. 12, adjacent hydrocarbon chains have the tightest packing in an all *trans* geometry when the C–C–C angles of adjacent chains are directly across from each other. That is, when a perpendicular line drawn from an atom on one chain intersects the corresponding atom on the adjacent chain. Only certain discrete tilt angles fulfill this condition. From the right-angle triangle which is shown at the bottom of Fig. 12, the condition is satisfied when

$$\tan\tau = \frac{nR}{D}, \quad n = 0,1,2,\ldots, \tag{12}$$

where τ is the tilt of the hydrocarbon chain from the surface normal, R is the distance between second nearest-neighbor carbon atoms along the chain (typically $R = 2.52$ Å), and D is the minimum separation between hydrocarbon chains which is typically $D = 3.6$ to 4.0 Å.[23] Clearly, if the chains are vertical ($\tau = 0°$ and $n = 0$) then any separation between chains satisfies Eq. (12). Cd arachidate is an example of this type of packing. If the chains are tilted, however, then crowding between the chains becomes important and only certain angles are allowed. For example, Eq. (12) predicts a tilt angle of 32° to 35° with $n = 1$, a tilt of 51° to 54° with $n = 2$, a tilt of 62° to 64° with $n = 3$, a tilt of 68° to 70° with $n = 4$, and a tilt of 72° to 74° with $n = 5$. The case of $n = 1$ is in good agreement with the 33° tilt angle determined for Ca arachidate. Thus Cd and Ca arachidate satisfy Eq. (12) with values of $n = 0$ and 1, respectively.

This microscopic model further predicts that the coverages of the LB film should decrease as the tilt of the hydrocarbon chains increase which is qualitative agreement with observations. From the bottom of Fig. 12, it is apparent that if the perpendicular distance between chains D is fixed, the base B of the right angled triangle which is parallel to the surface increases as the tilt of the hydrocarbon chain increases. This implies that as the hydrocarbon chains tilt the separation between chains along the surface increases or that the coverage decreases. Also, for tilted chains the coverage is expected to be lower because at domain boundaries there is a reduced density. Experimentally this is observed since the relative coverages of Cd arachidate, Ca arachidate, and arachidic acid are 1.0, 0.65, and 0.15, respectively, as measured from the heights of the edge jumps after the spectra are normalized to the same value immediately below the edge. Thus it is seen that the coverages of Cd and Ca arachidate as well as the detailed angular dependence study above, indicate that the hydrocarbon chains of Ca arachidate are tilted more than that of Cd arachidate.

The angular dependence and coverage of the arachidic acid suggest that the hydrocarbon chains are disordered. As discussed with Eq. (6b) the isotropy of the C–C σ^* resonance could be attributed to disorder chains or fortuitous tilts of the hydrocarbon chain near 71°. In order for the C–H* resonance to be isotropic, however, Eq. (8) indicates that the tilt of the arachidic acid chain would have to be nearly 90°. Thus the requirements for isotropy of the C–C σ^* and C–H* resonances are different suggesting that the hydrocarbon chains of arachidic acid are actually disordered. The low relative coverage of arachidic acid vs that of the ordered layers of Ca and Cd arachidate also seems consistent with disordered hydrocarbon chains. This disorder may be the result of the difference in the carboxyl group which for the salts is stripped of its hydrogen atom but is intact in the acid. Therefore, for the salt both oxygens can contribute to

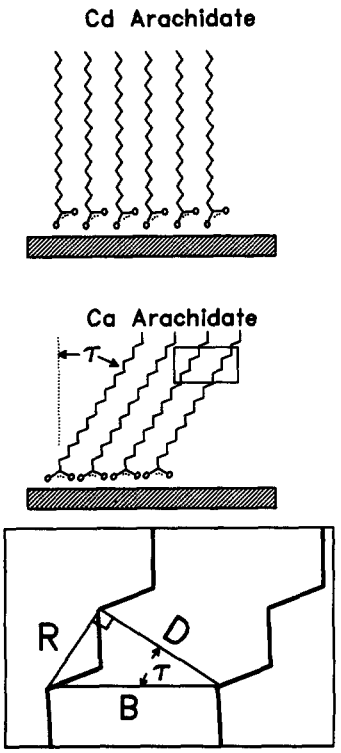

FIG. 12. Packing of hydrocarbon chains and quantum tilt model. Proposed models for the hydrocarbon chain orientation of films of cadmium and calcium arachidate. The cadmium arachidate chains are nearly normal to the surface (top), while the calcium arachidate chains are tilted by 33°. At the bottom is shown how efficient packing of the chains depends upon the tilt angle and separation between chains.

the surface bond while in the acid hydrogen bonding to the surface and/or, more likely, between the molecules is expected to be important.

Several other aspects of the structure of the LB chains on Si(111) are apparent from the NEXAFS spectra. First, while the differences in orientation of the hydrocarbon chains observed for the various films is largely attributed to conditions during transfer of the films, the cation involved and the bonding of the arachidate chain to it may also be important. Indeed, Fig. 12 suggests that Cd arachidate with its vertical chain is bonded to the surface with only *one* oxygen atom, while Ca arachidate with its tilted chain is almost perfectly chelated with both oxygens on the surface. Of course, kinks in the chain near the carboxylate group might change this geometry somewhat. Thus, precisely how the carboxylate group bonds to the surface and how it accomodates differences in the orientation of the hydrocarbon chain remain interesting questions. The second aspect of the geometry indicated by these results is that the hydrocarbon chains are immobile and not able to freely spin about their axis. This is, the tilted-chain model is favored over the spinning-chain model in explaining the angular dependence of the three major NEXAFS resonances. One reason against the spinning-chain model is the small 24.7° to 25.4° tilt angle it predicts for Ca arachidate which is about 8° less than that predicted by the microscopic model above. It is also hard to understand how the carboxylate group of Ca arachidate could be coordinated to the surface if the chain is allowed to spin about its axis (Fig. 12).

The results of this NEXAFS study are in general agreement with previous studies regarding the orientation of LB films. For example, previous studies of the orientation of Cd arachidate multilayers on silver and silver bromide substrates found that the hydrocarbon chains were oriented nearly normal to those surfaces just like on the Si(111) surface of this study.[4] Also, on glass waveguides a perpendicular orientation of the hydrocarbon chains was found.[5] Indeed, it seems as if these are not epitaxial films since the orientation is considered to be independent of the substrate.[24]

The second major result of this study is the guidelines it establishes for the quantitative analysis of NEXAFS spectra. In particular, the descriptions of the line shapes of the various NEXAFS peaks and the description of the absorption step caused by ionization to states in the continuum. In several cases a physical reason can be given for the choice of the particular function used or of the parameter derived. There are several examples of this. (1) The C–H* resonance is Gaussian in shape because its width is near that of the resolution of the monochromator. (2) The shape of the absorption step to the continuum is based upon the convolution of a Gaussian peak and a vertical step. (3) The position of the inflection point of the step which was derived in this work so that the angular dependence of the C–H* resonance was consistent with that of the C–C σ^* resonance, was 287.6 eV. This value suggests that the absorption step is due to transitions from the C 1*s* level to the CBM (conduction band minimum) of a long hydrocarbon chain. For comparison, the binding energy of the C 1*s* level relative to the CBM has been measured by photoemission to be 288.5 $\pm$ 0.3 eV for polyethylene.[25] This energy is 0.9 eV higher than the inflection point which we measure, but we expect a difference because of excitonic transitions just below the edge which could not be resolved with our monochromator resolution. Such excitonic levels have been resolved in the near-edge spectrum of diamond.[19] These excitonic levels may also distort the width of the step since a width of 2.83 eV had to be used to obtain a reasonable fit whereas the monochromator resolution is about 1.2 eV.

Finally, this work reinforces the principle that NEXAFS spectra can generally be described as the superposition of the features from the constituent bonds of the system being studied. In particular, the C–C σ^* resonance can be described as due to resonances with *noninteracting* C–C antibonding orbitals. This differs from the case of valence-level excitation of hydrocarbons where extensive interaction occurs which is apparent as a splitting of the valence levels resulting in a series of transitions.[17,18] In the core-level excitation spectra observed here, however, there is no splitting of the C–C σ^* resonance position and the polarization dependence follows that of the individual C–C σ^* orbitals. This is also predicted by $X\alpha$ multiple scattering calculations for propane.[14] This noninteracting model for antibonding orbitals has generally been observed to be followed in the NEXAFS spectra of molecules containing different types of bonds. For example, the NEXAFS spectra of polyfunctional molecules can largely be explained as a superposition of features of the individual functional groups.[21] The only known exception to this superposition principle is the case of conjugated π bonds.[21,26]

VI. CONCLUSIONS

In this study the orientations of arachidate LB films on Si(111) are examined. Cd and Ca arachidate films form well ordered layers where the hydrocarbon chains are estimated to be tilted by 0° and 33°, respectively. These tilt angles are the result of packing considerations for the hydrocarbon chains which can be predicted from a simple geometric model. Arachidic acid, in contrast, forms disordered layers.

In addition, a quantitative approach toward the analysis of NEXAFS spectra is developed using least-squares fitting of difference spectra and the original NEXAFS spectra. This approach demonstrates that the NEXAFS spectra of hydrocarbon chains are similar with respect to the number, positions, widths, and line shapes of the NEXAFS features, regardless of the type of molecule or environment in which the hydrocarbon chain is located. Furthermore, the NEXAFS spectra are well described by a noninteracting C–C bond model in contrast to the case of valence level UV absorption spectra.

ACKNOWLEDGMENTS

We would like to thank Michael Philpott and Paul Bagus of IBM Almaden Research Center for valuable discussions regarding the interpretation of the spectra. We would also like to thank B. Hermsmeier, H. H. Rotermund, P. Stevens, and J. Solomon for help with the measurements. This

work was done at the Stanford Synchrotron Radiation Laboratory which is supported by the Office of Basic Energy Sciences of DOE and the Division of Materials Research of NSF.

[1]K. B. Blodgett and I. Langmuir, Phys. Rev. **51**, 964 (1937).
[2]G. L. Gaines, Jr., *Insoluble Monolayers at Liquid–Gas Interfaces* (Wiley–Interscience, New York, 1966), Chap. 8.
[3]See *Thin Solid Films* **132–134** (1985).
[4]J. F. Rabolt, F. C. Burns, N. E. Schlotter, and J. D. Swalen, J. Chem. Phys. **78**, 946 (1983).
[5]J. P. Rabe, J. D. Swalen, and J. F. Rabolt, J. Chem. Phys. **86**, 1601 (1987).
[6] S. Garoff, H. W. Deckman, J. H. Dunsmuir, M. S. Alvarez, and J. M. Bloch, J. Phys. (Paris) **47**, 701 (1986).
[7]M. Seul, P. Eisenberger, and H. M. McConnell, Proc. Natl. Acad. Sci. U.S.A. **80**, 5795 (1983).
[8]D. P. E. Smith, A. Bryan, C. Quate, J. Rabe, Ch. Gerber, and J. D. Swalen, Proc. Natl. Acad. Sci. U.S.A. **84**, 969 (1987).
[9]J. Stöhr and R. Jaeger, Phys. Rev. B **26**, 4111 (1982).
[10]F. Sette, J. Stöhr, and A. P. Hitchcock, J. Chem. Phys. **81**, 4906 (1984).
[11]J. Stöhr, in *X-ray Absorption: Principles, Applications, Techniques of EXAFS, SEXAFS and XANES*, edited by D. C. Koningsberger and R. Prins (Wiley, New York, 1988).
[12]A. P. Hitchcock and I. Ishii, J. Electron Spectrosc. **42**, 11 (1987).
[13]A. P. Hitchcock, D. C. Newbury, I. Ishii, J. Stöhr, J. A. Horsley, R. D. Redwing, A. L. Johnson, and F. Sette, J. Chem. Phys. **85**, 4849 (1986).
[14]J. Stöhr, D. A. Outka, K. Baberschke, D. Arvanitis, and J. A. Horsley, Phys. Rev. B **36**, 2967 (1987).
[15]J. Stöhr and D. A. Outka, Phys. Rev. B **36**, 7891 (1987).
[16]The C–C–C bond angles of a long hydrocarbon chain molecule are typically somewhat larger than the ideal tetrahedral angle of 109.5°. For example, in the structure of potassium palmitate the average angle is 114.4°: J. H. Dumbleton and T. R. Lomer, Acta. Crystallogr. **19**, 301 (1965).
[17]J. W. Raymonda and W. T. Simpson, J. Chem. Phys. **47**, 430 (1967).
[18]R. H. Partridge, J. Chem. Phys. **52**, 2485 (1970).
[19]J. F. Morar, F. J. Himpsel, G. Hollinger, G. Hughes, and J. L. Jordan, Phys. Rev. Lett. **54**, 1960 (1985).
[20]J. A. Horsley, J. Chem. Phys. **76**, 1451 (1982).
[21]D. A.Outka, J. Stöhr, R. J. Madix, H. H. Rotermund, B.Hermsmeier, and J. Solomon, Surf. Sci. **185**, 53 (1987).
[22]J. Stöhr, D. A. Outka, K. Baberschke, D. Arvanitis, and J. A. Horsley, Phys. Rev. B **36**, 2967 (1987).
[23]C. W. Bunn, Trans. Faraday Soc. **35**, 482 (1939).
[24]V. Vogel, and Ch. Wöll, J. Chem. Phys. **84**, 5200 (1986).
[25]J. Delhalle, J. M. André, S. Delhalle, J. J. Pireaux, R. Caudano, and J. J. Verbist, J. Chem. Phys. **60**, 595 (1974).
[26]J. A. Horsley, J. Stöhr, A. P. Hitchcock, D. C. Newbury, A. L. Johnson, and F. Sette, J. Chem. Phys. **83**, 6099 (1985).